JOURNAL OF MATERIALS SCIENCE 16 (1981) 1533–1547

The influence of reinforcing fibres on the growth of cracks in brittle matrix composites

Y. KORCZYNSKYJ, S. J. HARRIS, J. G. MORLEY
Department of Metallurgy and Materials Science, and Wolfson Institute of Interfacial Technology, University of Nottingham, Nottingham, UK

The use of fibres to improve the work-of-fracture and strength of brittle matrices has gained interest in a number of fields, especially in the cement and plaster industry, and also in high-temperature applications of ceramics and glasses. Here a theoretical analysis is presented to account for the enhanced strain-to-failure values of a brittle matrix containing microcracks and reinforced with fibres. The theory assumes that the Griffith energy criterion for failure applies when a crack is present in the matrix. It predicts the stabilizing effect of a unidirectional uniform distribution of fibres which bridge a matrix crack by computing the rates of release of strain energy and of absorption energy with increasing length of a matrix crack. Published experimental data on the carbon fibre reinforced glass system is used to compare the predictions of the theory here with a version given by Aveston, Cooper and Kelly. Descriptions of the boundary conditions of single and multiple fracture are given. The theory is shown to further indicate the possible existence of an upper limit to the fibre volume fraction at which multiple fracture occurs, i.e. when the fibres stabilizing the crack cannot support the load. Applications of the analysis to the design of composite systems of technological importance are suggested.

1. Introduction

It has been shown that the incorporation of continuous brittle fibres into ceramic and glass matrices can produce a composite which has both improved strength and toughness. Experiments by Sambell *et al.* [1, 2], Phillips *et al.* [3] and more recently by Prewo and Bacon [4] on the use of carbon fibres to reinforce a number of different types of glass matrix have clearly demonstrated the effectiveness of such materials, e.g. the work-of-fracture can be increased from 10 to 10^3 J m^{-2}. In this type of composite the matrix has a lower failure strain than the fibres and this factor brings about microcracking in the glass phase at a much lower strain than that at which final catastrophic fracture occurs.

An attempt to analyse the effect of a unidirectional array of fibres on the cracking strain of a brittle matrix has been made by Aveston, Cooper and Kelly [5] (ACK theory). The approach taken was to compare the change in the potential energy of the composite material and loading system caused by the presence of a transverse matrix crack, with the work-of-fracture of the matrix material. Matrix fracture was assumed to occur during the application of a tensile load to the composite material if the matrix strain exceeded its failing strain in the unreinforced condition and provided also that there was a decrease in the potential energy of the composite specimen and the loading system. According to this analysis the unreinforced matrix failure strain will be enhanced to a value of ϵ_{muc}, where,

$$\left(\frac{12\tau E_f V_f^2 \gamma_m}{E_c E_m^2 V_m r}\right)^{-\frac{1}{3}} = \epsilon_{muc}, \quad (1)$$

where E_f, E_m and E_c are, respectively, the

0022–2461/81/061533–15$03.50/0

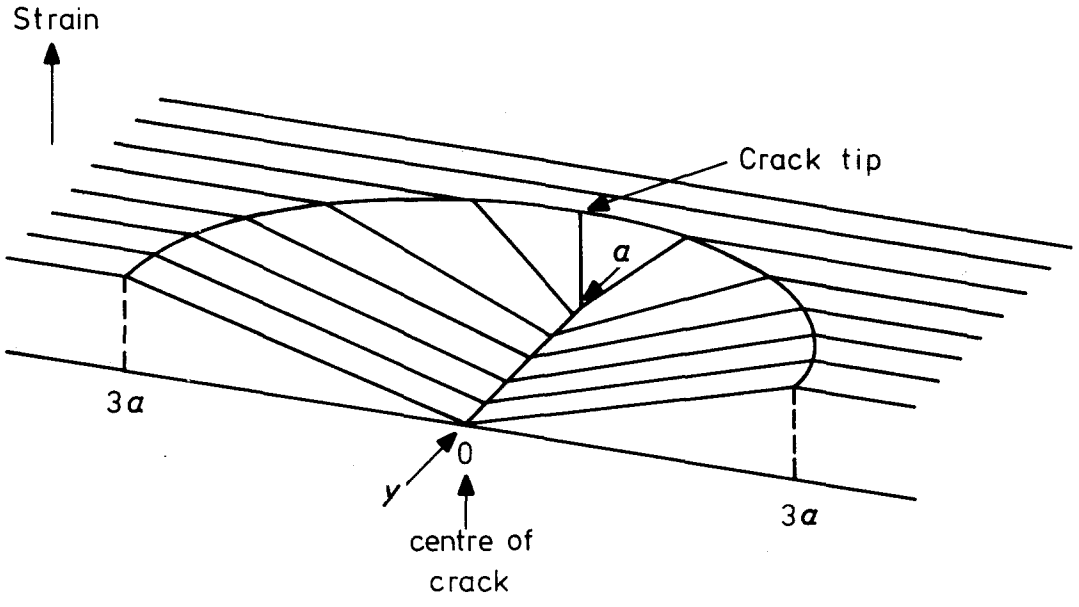

Figure 1 Idealized strain distribution around a crack in an unreinforced sheet.

Young's modulus of fibre, matrix and composite, V_f and V_m are the volume fractions of fibre and matrix and γ_m is the fracture energy of the matrix.

If the value of ϵ_{muc} predicted from Equation 1 is less than ϵ_{mu}, the failing strain of the unreinforced matrix, the fibres are assumed not to modify the matrix failure strain. If the fibre diameter, $2r$, is sufficiently small and τ, the shear strength of the fibre matrix interface, is sufficiently large, the matrix will fracture at a value of ϵ_{muc} greater than that for the unreinforced material, ϵ_{mu}. Thus the theory predicts an enhancement of the matrix failing strain if a sufficient volume fraction of appropriate fibrous material is incorporated within it. The above argument does not consider the mechanics of crack growth and only two conditions are considered: the uncracked condition and the situation in which a crack has propagated completely across the specimen.

In the analysis described here an alternative physical model is considered. Cracks must be present in any brittle matrix and the Griffith energy criterion for failure is assumed to control the matrix strength. The model is based on a previous analysis [6–8] dealing with the mechanics of transverse matrix crack growth in reinforced systems containing continuous crack-bridging reinforcing members. It is limited to a consideration of a unidirectional uniform distribution of fibres which are aligned at right angles to the crack axis. The fibres are assumed to be circular in section and to be bonded frictionally to the matrix, the interface having a constant shear strength value. A feature of the model is its ability to predict the stabilizing effects of fibres on matrix cracks where these control the failing strain of the matrix. The unreinforced matrix is therefore the end point of a continuous relationship which describes the effect of an increasing volume fraction of reinforcing fibres on unstable crack extension in the matrix.

The predictions of the analysis of various changes in the physical characteristics of the component parts of the composite structure are illustrated and compared with those of the ACK theory. In addition the correlation of the analysis with experimental behaviour of carbon fibre reinforced glass is examined.

2. The influence of crack bridging fibres on the growth of a matrix crack

The physical model and analytical procedures used to describe the effect of various factors on the mechanics of crack growth have been described in detail elsewhere [6–8] and will only be covered in outline here. The strain field around a crack in the unreinforced matrix is assumed to approximate to the situation described in Fig. 1. The strain carried by the material in the vicinity of the crack is assumed to increase linearly along any line drawn in a direction perpendicular to the length of the crack from zero at the crack face to the value of bulk strain carried by the material at the edge of

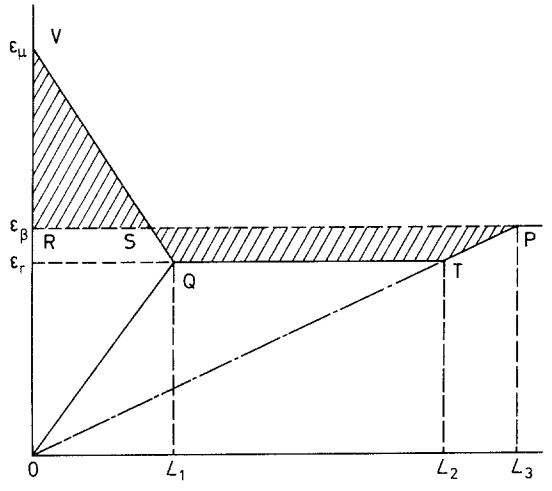

Figure 2 Assumed strain distributions within a section perpendicular to the crack face of a reinforced matrix.

an elliptical zone drawn around the crack. Strains, and associated strain energies, are considered only in the direction perpendicular to the crack face. The size of the elliptical zone is chosen so that the release of strain energy by the elastic relaxation of the material within the elliptical zone (calculated within the restrictions described above) is numerically the same as that calculated by integrating the strain field around a crack in an ideal isotropic elastic solid. It follows that the major axis of the elliptical zone is three times the crack length.

The strain field is modified by the presence of crack-bridging fibres which are assumed to be uniformly distributed and arranged perpendicular to the crack faces. Stress is transferred between the matrix and the fibres via the fibre–matrix interface which is assumed to have a constant shear strength value. Fig. 2 shows the strain distribution within the reinforcing fibres and the matrix within a section of the ellipitical zone perpendicular to the crack face. The slopes of the lines VQ and OQ are the gradients of strain in the fibres and matrix and are given respectively by

$$\frac{d\epsilon_f}{dx} = \frac{-2\tau}{E_f r}, \tag{2}$$

and

$$\frac{d\epsilon_m}{dx} = \frac{2V_f\tau}{E_m V_m} + \frac{\epsilon_\beta}{L_3}, \tag{3}$$

where ϵ_f is the strain carried by a fibre and ϵ_m is the strain carried by the adjacent matrix at any arbitrary distance x from the crack face. The gradient of strain in the matrix, $d\epsilon_m/dx$, along the section in the absence of the reinforcing fibres is ϵ_β/L_3, where ϵ_β is the general tensile strain carried by the material outside the elliptical zone as a consequence of a uniform tensile stress applied at right angles to the length of the crack. Since changes in strain are assumed to be confined within the elliptical zone then the length of the fibres extending across the elliptical zone, which surrounds the crack, must be the same as their length in the absence of a crack. It follows that the two areas shown shaded in Fig. 2 must be the same since these are proportional to the amounts by which different portions of a reinforcing fibre have extended and contracted within the elliptical zone. This enables the values of ϵ_μ, ϵ_r, L_1, L_2 and L_3, illustrated in Fig. 2, to be defined,

$$\begin{aligned} \epsilon_r &= \epsilon_\beta L_3/[Q(P+\epsilon_\beta/L_3)^{-2} + L_3/\epsilon_\beta]^{\frac{1}{2}}; \\ \epsilon_\mu &= L_1(P+Q+\epsilon_\beta/L_3); \\ L_1 &= \epsilon_r(P+\epsilon_\beta/L_3)^{-1}; \\ L_2 &= L_3\epsilon_r/\epsilon_\beta, \end{aligned} \tag{4}$$

where $P = 2V_f\tau/E_m V_m r$ and $Q = 2\tau/E_f r$. Also if y is the distance from the centre of the crack to the segment considered and a is the half-crack length then

$$L_3 = 3(a^2 - y^2)^{\frac{1}{2}}. \tag{5}$$

The half-crack opening at a distance y from the centre of the crack is obtained from the difference in integrated strain between the reinforcing fibres and the matrix over the distance OL_1 and is given by

$$\mu = \epsilon_\mu L_1/2. \tag{6}$$

Equation 4 enables the strain field within the elliptical zone to be defined. The development of the strain field as the length of a matrix crack increases is indicated by the sequence (a), (b), (c) and (d) in Fig. 3. The same pattern of change in the strain field would also be obtained if the crack length was fixed and progressive reductions in the diameter of the crack-bridging fibres was considered. It is interesting to note that the strain carried by the fibres bridging the crack can be appreciably greater than the strain carried by the fibres elsewhere in the system, hence, a matrix flaw can initiate fibre failure in certain circumstances.

From Equation 4 the strain energy released, δWR_y, by a parallel-sided segment of composite material within the elliptical zone and situated at a distance y from the centre of the crack can be determined

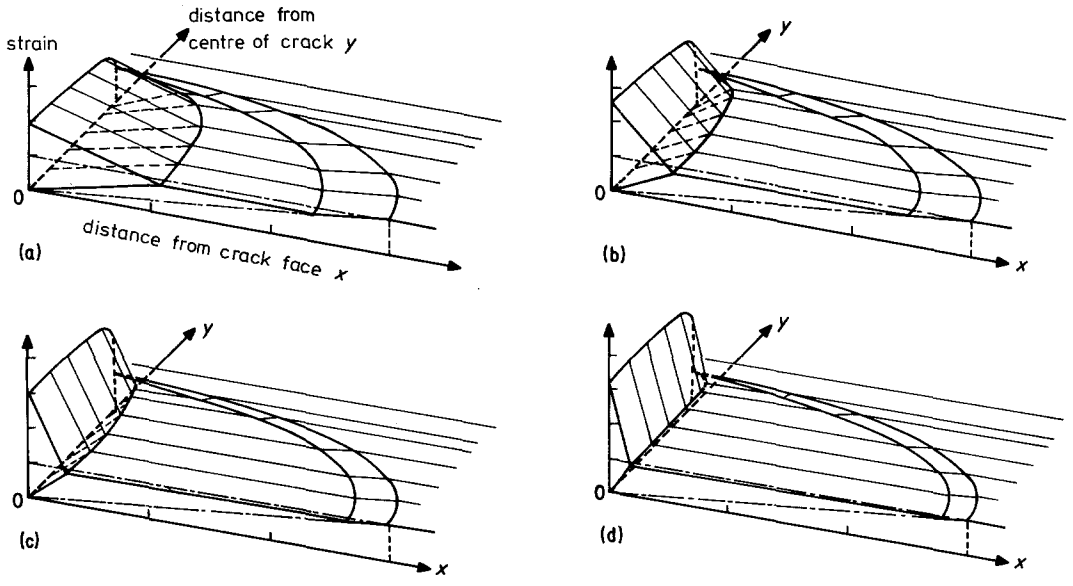

Figure 3 Development of strain field with increasing crack length.

$$\delta WR_y = [E_c\epsilon_\beta^2 L_3/2 - E_c\epsilon_\beta^2(L_3^3 - L_2^3)/6L_3^2 - E_c\epsilon_f^2(L_2 - L_1)/2 - V_m E_m \epsilon_r^2 L_1/6 - V_f E_f(\epsilon_\mu^2 + \epsilon_\mu\epsilon_r + \epsilon_r^2)L_1/6]\delta y, \quad (7)$$

where $E_c = E_m V_m + E_f V_f$.

The total strain energy released as a consequence of the matrix crack can be computed by numerically integrating Equation 7 over the whole of the elliptical zone. This has been done by dividing a quadrant of the ellipse into a number of zones of equal width which are summed to give the energy released over the entire quadrant (see Section 3.1). The strain energy released for incremental increases in crack length is then obtained and the rate of release of strain energy with increasing crack length calculated by numerical differentiation.

If a frictional bond is assumed between fibre and matrix, work is done against frictional losses as the crack extends. This follows because within the stress transfer zone near the matrix crack faces the reinforcing fibres are elongating elastically whilst the matrix surrounding them is relaxing.

The relative displacement dm_x at a distance x from the crack face is given by the integrated strain difference between the fibre and the matrix from the position x to L_1 so that

$$dm_x = \int_x^{L_1} \epsilon_\mu(1 - x/L_1)\,dx = \epsilon_\mu(L_1/2 - x + x^2/2L_1). \quad (8)$$

The frictional force acting over a length dx of the fibre is given by $2\pi r\tau\,dx\,dm_x$.

The total work done is obtained by integrating this expression from 0 to L_1 and is

$$\pi r\tau\epsilon_\mu L_1^2/3. \quad (9)$$

Since the number of fibres in a section of width δy and unit thickness is $V_f\delta y/\pi r^2$ the work done against frictional forces in this segment of the quadrant is

$$\delta WA_y = V_f\tau\epsilon_\mu L_1^2\delta y/3r. \quad (10)$$

Substituting for ϵ_μ from Equation 4 gives

$$\delta WA_y = V_f\tau\delta y\{P + Q + \epsilon_\beta/L_3\}L_1^3/3r. \quad (11)$$

The total energy absorbed frictionally is then obtained by numerically integrating Equation 11 over the quadrant of the ellipse and the rate of frictional absorption of energy with increasing crack length is obtained by numerically differentiating values obtained for incremental increases in crack length.

Energy is also absorbed in rupturing the matrix by the creation of new surfaces and in associated energy absorbing mechanisms. This can be assumed to have a constant value G_c which has to be added to the frictional energy loss term to arrive at the total work done in propagating a matrix crack.

Hence the rate of release of strain energy and the rate of absorption of energy with increasing length of a matrix crack length can be calculated

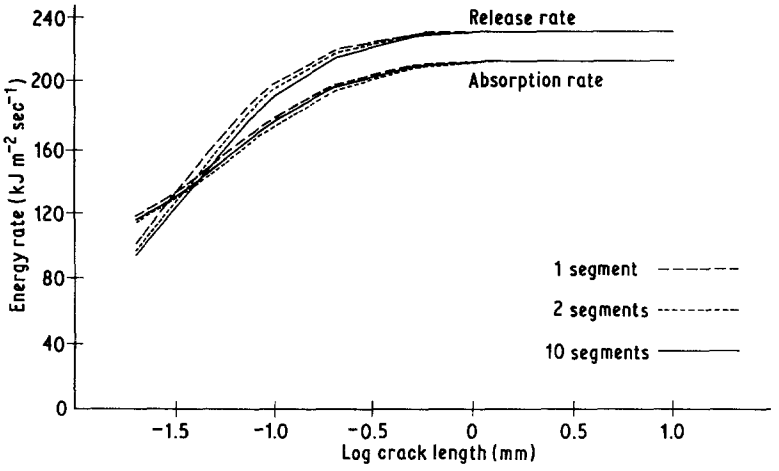

Figure 4 Rates of release and absorption of strain energy with increasing crack length shown as a function of the number of parallel segments into which the elliptical strain field around the matrix crack has been divided. ($\tau = 3\,\mathrm{MN\,m^{-2}}$, $\epsilon_\beta = 0.28\%$, $V_f = 50\%$, $2r = 8\,\mu\mathrm{m}$, $G_c = 8\,\mathrm{J\,m^{-2}}$, $E_m = 70\,\mathrm{GN\,m^{-2}}$, $E_f = 380\,\mathrm{GN\,m^{-2}}$).

for any unidirectionally reinforced fibrous composite in which the fibres have a higher failing strain than the matrix and bridge a matrix crack orthogonally. Unstable growth of the matrix crack will occur when the rate of release of strain energy with increasing crack length is greater than the rate of energy absorption.

3. Application of the model to the fracture behaviour of a carbon fibre reinforced brittle matrix system

The model predicts that various types of failure processes will occur and that these will be influenced by the physical characteristics of the component parts of the composite structure. This is illustrated below. Comparisons are also made between the predictions of this model and the one previously put forward by Aveston, Cooper and Kelly [5]. Pyrex glass unidirectionally reinforced with carbon fibres has been used for these calculations and the physical properties taken for this system are those used by Aveston, Cooper and Kelly [5]. The elastic modulus of the pyrex matrix, E_m, being taken as $70\,\mathrm{GN\,m^{-2}}$, the elastic modulus of the carbon reinforcing fibres, E_f, being taken as $380\,\mathrm{GN\,m^{-2}}$, the work-of-fracture of the matrix G_c (twice the surface energy γ) being taken as $8\,\mathrm{J\,m^{-2}}$, and the unreinforced matrix failing strain, ϵ_{mu}, being taken as 0.14%. It will be noted that rather different values for these properties are given in a later paper by Sambell *et al.* [2].

The length of the cracks $2a$, assumed initially to be present in the matrix, are calculated on the basis of the Griffith equation

$$G_c = \pi a E_m \epsilon_{mu}^2 \qquad (12)$$

so that the length, $2a$, of the cracks pre-existing in the matrix is $37.2\,\mu\mathrm{m}$. These cracks are assumed to be bridged transversely by the reinforcing carbon fibres, which remain intact. The composite strain values, ϵ_β, at which composite failure would occur by various failure mechanisms have been calculated. The effects of fibre volume fraction, fibre thickness, fibre–matrix interfacial shear strength, the flaw size (and hence strength of the unreinforced matrix) and the effect of significant increases in the matrix work of fracture are illustrated. The data presented therefore describe the expected behaviour of pyrex glass unidirectionally reinforced with carbon fibres and illustrate the effects which might be expected, on the basis of the theory, by changing various physical parameters in this system.

3.1. Factors to be considered in establishing the physical validity of the theoretical model

In the analysis set out in Section 2 of this paper the elliptical zone was assumed to be divided into a finite number of parallel segments, each perpendicular to the length of the crack. The strain energy released and absorbed in each of these segments is summed over the whole of the elliptical zone and numerically differentiated for increments in crack length to give the computed rate of release and absorption of energy with increasing crack length. In the case of most of the computations the elliptical zone has been divided into ten segments. In Fig 4 the elliptical zone has been divided into various numbers of segments and the strain energy release and absorption rates with increasing crack length have been computed for one particular system. The results indicated in Fig. 4 are typical of other systems. It is apparent that the numerical predictions of the analytical

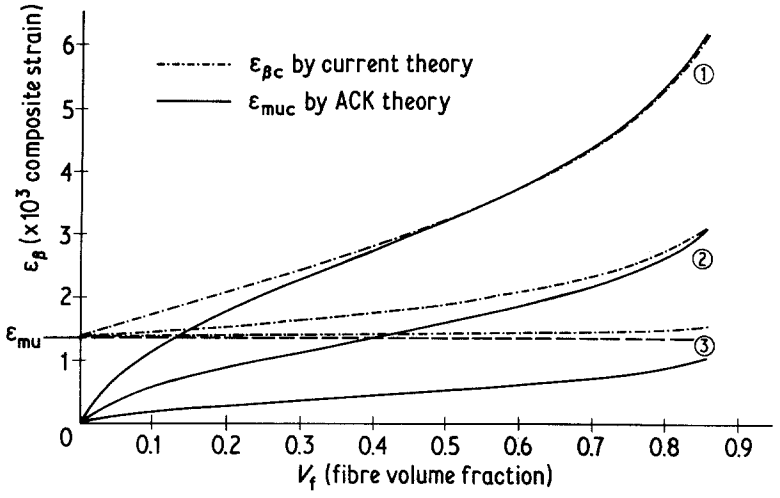

Figure 5 Effect of fibre diameter $2r$, on the strain for matrix crack extension ϵ_c against fibre volume fraction. (Curve (1) $2r = 1\,\mu$m, curve (2) $2r = 8\,\mu$m, curve (3) $2r = 100\,\mu$m). Calculations of all plots assume $\tau = 2\,\text{MN m}^{-2}$, $\epsilon_{mu} = 0.0014$, $G_c = 8\,\text{J m}^{-2}$, $E_m = 70\,\text{GN m}^{-2}$, $E_f = 380\,\text{GN m}^{-2}$. ACK theory indicated by lower curve in all cases.

model change as the number of segments into which the elliptical zone is divided is reduced. However, above ten segments no significant change takes place and it is not until the number of segments is reduced to less than about five that small differences arise. Thus the model appears to be able to predict the rates of release and absorption of energy as a function of crack length when the crack is bridged by a small number of fibres with an accuracy equivalent to that associated with crack-bridging by a large number of fibres. This point is of some significance in the case of the carbon fibre pyrex glass composite structure because cracks about $40\,\mu$m in length will be bridged by about five $8\,\mu$m diameter carbon fibres when these are present at a volume fraction of 30% and arranged in a uniform hexagonal array. Hence the predictions of the theory do not seem likely to be seriously in error, from this source, for $8\,\mu$m diameter carbon fibres at volume fractions of 30% and above (see Fig. 5). The enhancement of the composite strain predicted for fibre volume fractions less than 30% is in any case very small so that, even at lower fibre volume fractions than 30%, the errors from this source again do not seem likely to be significant compared with the other approximations used in the development of the analysis.

3.2. Comparison of theoretical models

In the case of the data presented in Fig. 5, the effect of fibre volume fraction on the matrix failing strain is shown for three fibre diameters, 1.0, 8 and $200\,\mu$m. Also shown in Fig. 5 are the results predicted by the ACK analytical model. The latter analysis is limited to a consideration of the energetics of the formation of a crack which extends across the full width of a specimen, (Equation 1). The analysis is only relevant when it predicts a composite cracking strain greater than that of the unreinforced matrix. It is apparent from Fig. 5 that for the $8\,\mu$m diameter carbon fibre pyrex glass system the ACK analysis predicts that an enhancement of the matrix failing strain will occur for this particular combination of composite properties only at high fibre volume fractions, when a lower interfacial shear strength value, τ, of $2\,\text{MN m}^{-2}$ is assumed. It is interesting to note that at very high fibre volume fractions the cracking strain of the matrix predicted by the ACK analysis approaches the values derived from the argument put forward here.

3.2.1. Effect of fibre diameter

It is apparent from Fig. 5 that the predictions of the two analyses approach each other at very high fibre volume fractions for $8\,\mu$m diameter fibres. For $1\,\mu$m diameter fibres the predictions of the two analyses become indistinguishable at fibre volume fractions of about 50%. The thinner fibres enhance the composite strain at which existing matrix cracks become unstable by a greater amount than the $8\,\mu$m fibres. By contrast fibres of much greater diameter ($200\,\mu$m) have little influence on the matrix failing strain according to the analysis developed here. For fibres of this thickness the ACK analysis does not predict any enhancement in the matrix failing strain over the whole range of fibre volume fractions and there is a significant difference between the predictions of the two theories even at very high fibre volume fractions.

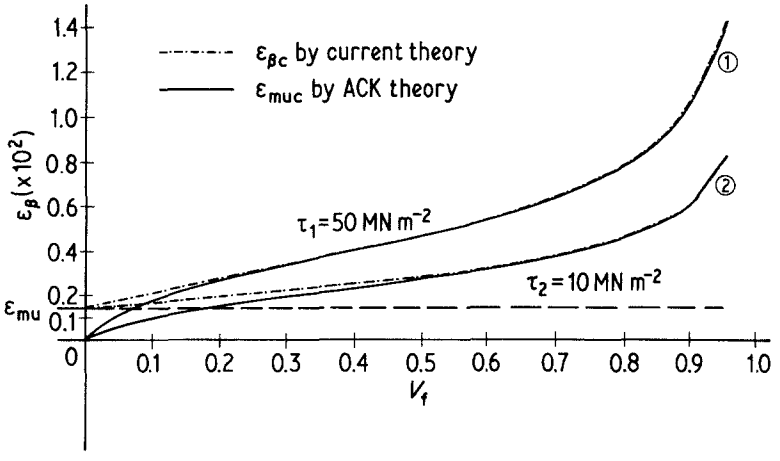

Figure 6 Effect of fibre–matrix interfacial shear strength on unstable matrix crack extension. Calculations of all plots assume $\epsilon_{mu} = 0.0014$, $G_c = 8\,J\,m^{-2}$, $E_m = 70\,GN\,m^{-2}$, $E_f = 380\,GN\,m^{-2}$.

The analysis developed here predicts a continuous relationship between the fibre volume fraction and the matrix failing strain extending over the whole range of fibre volume fractions. As discussed above, there is some uncertainty as to the validity of the analysis at very low fibre volume fractions (except when the fibre diameters are very small) since for this condition, it is apparent that the basis of the physical argument (the presence of a large number of fibres bridging the crack) does not apply when the flaw is small and the fibres are relatively large and widely spread. However, it is apparent that the predicted enhancement of the failing strain of the matrix for these conditions is very small. Both the ACK analysis and that put forward here predict a very considerable enhancement of the matrix failing strain when fibres of a very small diameter are present at an appreciable volume fraction.

3.2.2. Effect of changes in interfacial shear strength

In Fig. 6 the effect of increasing the shear strength of the frictional interface, τ, on the composite strain at which the intrinsic matrix cracks propagate, is shown as a function of fibre volume fraction, V_f, for a constant fibre diameter of 8 μm. Taken together with the data for this fibre diameter in Fig. 5, this illustrates the increase in the strain, ϵ_β, which the matrix would be expected to support as a consequence of increases in interfacial shear strength. Again for fairly high enhancement of matrix failing strain the present theory and that of ACK predict similar failing strains.

3.2.3. Effect of varying the matrix flaw size

Fig. 7 shows the predicted effect of increasing the half-length, a, of the inherent flaws in the matrix to 100 and 2000 μm, (with a concomittent reduction in the failing strain of the unreinforced matrix, since G_c is maintained constant at $8\,J\,m^{-2}$). As would be expected, the numerical values of strain enhancement with increasing fibre volume fractions for a matrix containing intrinsic flaws of length 200 μm is intermediate between the values for 37.2 and 4000 μm flaws. The ACK theory predicts the same failure strain for all values

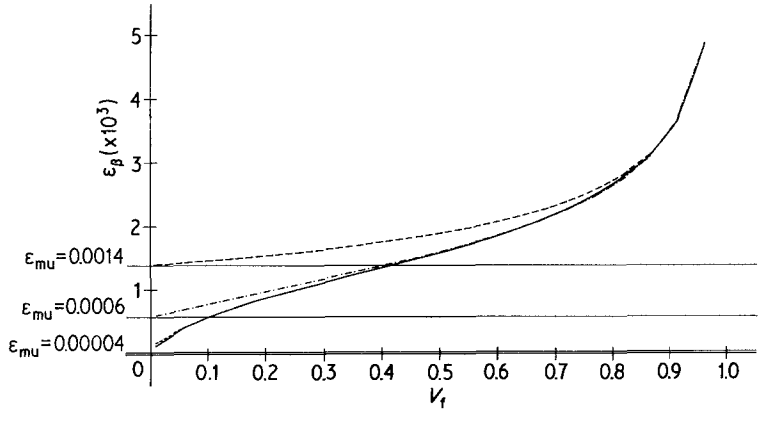

Figure 7 Effect of fibre volume fraction and the inherent matrix flaw size on the strain for unstable crack growth in the matrix. ($E_m = 70\,GN\,m^{-2}$, $E_f = 380\,GN\,m^{-2}$, $\tau = 2\,MN\,m^{-2}$, fibre diameter = 8 μm, $G_c = 8\,J\,m^{-2}$). (curve 1) $a = 18.6\,\mu m$, $\epsilon_{mu} = 0.0014$, (curve 2) $a = 100\,\mu m$, $\epsilon_{mu} = 0.0006$, (curve 3) $a = 2000\,\mu m$, $\epsilon_{mu} = 0.00004$. Predictions of ACK theory for zero matrix failing strain in curve (4).

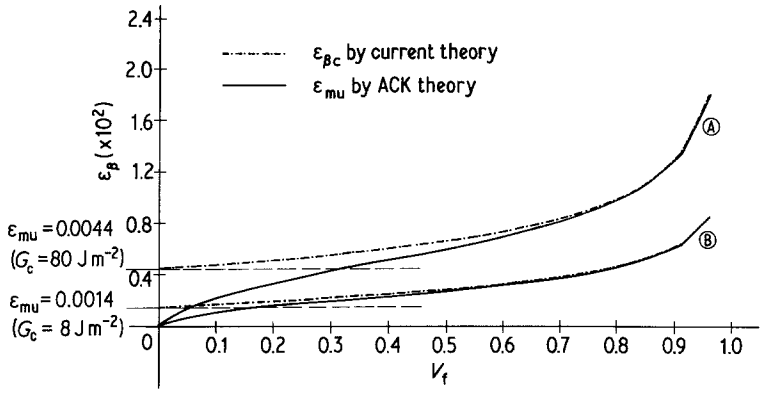

Figure 8 Effect of increasing the matrix work of fracture G_c on the matrix strain for unstable crack growth. Curve (A) G_c = 80 J m^{-2}, ϵ_{mu} = 0.0044, curve (B) G_c = 8 J m^{-2}, ϵ_{mu} = 0.0014. Calculations for all plots assume E_m = 70 MN m^{-2}, E_f = 380 MN m^{-2}, τ = 10 MN m^{-2}, d = 8 μm, a = 18.6 μm. Predictions of ACK theory shown by lower curves.

of a. Clearly the predictions of both models tend to converge as a approaches infinity.

3.2.4. Effect of matrix work of fracture

In Fig. 8 the effect, predicted by the present theory, of increasing the matrix work-of-fracture is shown. The intrinsic flaw size a is maintained at 18.6 μm and the fibre matrix interfacial shear strength is taken as 10 MN m^{-2}. The failure strain of the unreinforced matrix is, of course, increased, according to Griffith theory, by increasing the value of G_c by an order of magnitude, i.e. 8 to 80 J m^{-2}.

For this particular system the relative enhancement in matrix failure strain, over its unreinforced value, at a given fibre volume fraction is considerably higher at the low G_c value. The ACK theory and the present theory give similar predictions over a wide range of fibre volume fractions for the lower value of G_c but are only in agreement at very high fibre volume fractions for the higher G_c value.

3.2.5. Comparison between the ACK theory and the present theory

It is apparent from Figs 5, 6, 7 and 8, that both the ACK theory and the analysis set out here yield similar numerical predictions when the failing strain of a brittle matrix is enhanced very considerably by the presence of the fibres. Under these circumstances it also follows that a long crack remains stable at appreciable values of ϵ_β despite the low work-of-fracture of the matrix itself. For these conditions the strain energy released by matrix crack propagation is largely absorbed by frictional energy losses at the fibre–matrix interface and by the additional storage of strain energy by the crack-bridging fibres. The matrix work of fracture becomes an insignificant term in the energy balance relationship. For a given composite strain value, ϵ_β, the theory presented here predicts that the rate of release of strain energy and rate of absorption of strain energy approach limiting constant values with increasing crack length [7]. Hence, the matrix strain for unstable crack growth becomes insensitive to the absolute length of the crack when the mechanics of crack growth are primarily controlled by the presence of the fibres and fibre matrix interactions. The present analysis predicts a relatively constant separation between the faces of a long matrix crack [7]. This approximates to the situation considered in the ACK theory – a parallel-sided crack extending across the full width of the specimen. Hence in a regime in which (according to the present theory) the mechanics of crack growth are not significantly affected by the matrix work-of-fracture, and hence crack length, the physical arguments approximate to each other and both yield similar numerical values.

3.3. Single and multiple fracture conditions

So far the only failure criterion considered is the general tensile strain carried by the composite and the matrix at the point at which existing matrix flaws become unstable and propagate. Various other failure criteria impose boundary conditions on the failure of the composite and need to be considered. Some of the criteria impose catastrophic failure of the composite by the propagation of a local region of failure (single fracture). In other cases complete failure does not occur and multiple cracking of the matrix occurs. The criteria can be listed as follows:

(1) When the peak strain carried by the central fibre bridging the matrix crack as the crack becomes unstable is less than ϵ_{fu}, (the fibre failure strain) multiple matrix cracking will occur provid-

ing the fibres can support all of the load applied to the composite structure. However, as the volume fraction of fibres increases, the composite strain, ϵ_β, at which a given matrix crack will become unstable will increase. The strain carried by the fibres bridging the crack also increases and is higher than the general composite strain, (see Fig. 3) and the central crack-bridging fibres may reach their failing strain. As a consequence, a composite containing a flaw bridged by fibres can fail when the composite strain, ϵ_β, is less than the fibre failing strain. As the fibre volume fraction is increased, a point can be reached at which the centre fibre bridging the crack reaches its ultimate failing strain, ϵ_{fu}, at the same time as the matrix crack becomes unstable. Single fracture will then occur. This condition thus represents an upper limit for multiple matrix cracking. Also, if the peak strain carried by the central fibre bridging the crack reaches ϵ_{fu} before the matrix crack becomes unstable the composite will again fail catastrophically by single fracture thus imposing an alternative upper limit of ϵ_β for multiple matrix fracture.

(2) A second upper limit of fibre volume fraction for multiple matrix cracking can occur for the following reason. As the fibre volume fraction increases, the elastic strain and load which the composite structure can support is increased before matrix failure occurs by the propagation of existing flaws, i.e. the failing strain of the flawed matrix is increased and the stress carried by the composite is enhanced. If this increase is great enough, unstable fracture of the matrix can precipitate failure of the fibres because they may no longer be able to support the total load now applied to the composite structure. This will occur if the increase in the load bearing ability of the composite by the suppression of matrix crack growth, brought about by the presence of the fibres, is greater than the load bearing ability of the additional fibres introduced. It thus represents an alternative upper limit to the strain at which multiple matrix fracture will occur.

(3) If the fibres are present in low volume fractions and cannot support the total load applied to the composite structure after failure of the matrix, single fracture will occur. This condition thus represents a lower bound for multiple matrix cracking and has of course been identified previously (see for example [5]).

Thus, if the failure of the matrix is assumed to occur as a consequence of the unstable propagation of cracks bridged by fibres the analysis given here suggests that multiple matrix cracking will extend over a range of fibre volume fractions and have definite upper and lower bounds, the lower bound is unique and has previously been identified. The upper bound is set by the operation of two alternative mechanisms which can precipitate single fracture of the matrix. Whichever of these operates at the lower strain value will be critical for any particular system. Either mechanism may operate at the lower strain depending on the particular physical characteristics of the composite system considered. The onset of single fracture at high fibre volume fractions will, according to this analysis, take place at a composite strain less than the ultimate failing strain of the reinforcing fibres. Again the absolute value of this failing strain and the fibre volume fraction at which it will occur will depend on the particular physical characteristics of the system considered.

It appears that the most important single factor governing the fracture behaviour discussed above is the diameter of the fibres in relation to the length of the inherent matrix cracks. It is apparent from Fig. 5 that when the fibre diameters are large they enhance the strain at which existing matrix cracks become critical by only a very small amount. Hence, the load supported by the matrix when the existing cracks become critical is not increased significantly by the fibres so that the failure mechanism discussed under (2) above would not be relevant. Also the enhanced strain carried by the fibre bridging the centre of the crack would not be increased significantly over the general strain carried by the composite. Therefore, failure by the mechanism described under (1) above would not be apparent for composites having these characteristics. For these conditions multiple matrix cracking will occur up to the highest feasible fibre volume fractions.

The issues discussed above are illustrated in Fig. 9. Here the physical parameters are chosen primarily to illustrate the failure conditions considered but are similar to those in the carbon fibre reinforced glass system. The value of τ is taken as $10\,MN\,m^{-2}$ and $G_c = 20\,J\,m^{-2}$. Curve 1 illustrates the increasing matrix strain at which the intrinsic matrix flaw length ($a = 18.6\,\mu m$) becomes critical as the fibre volume fraction is increased.

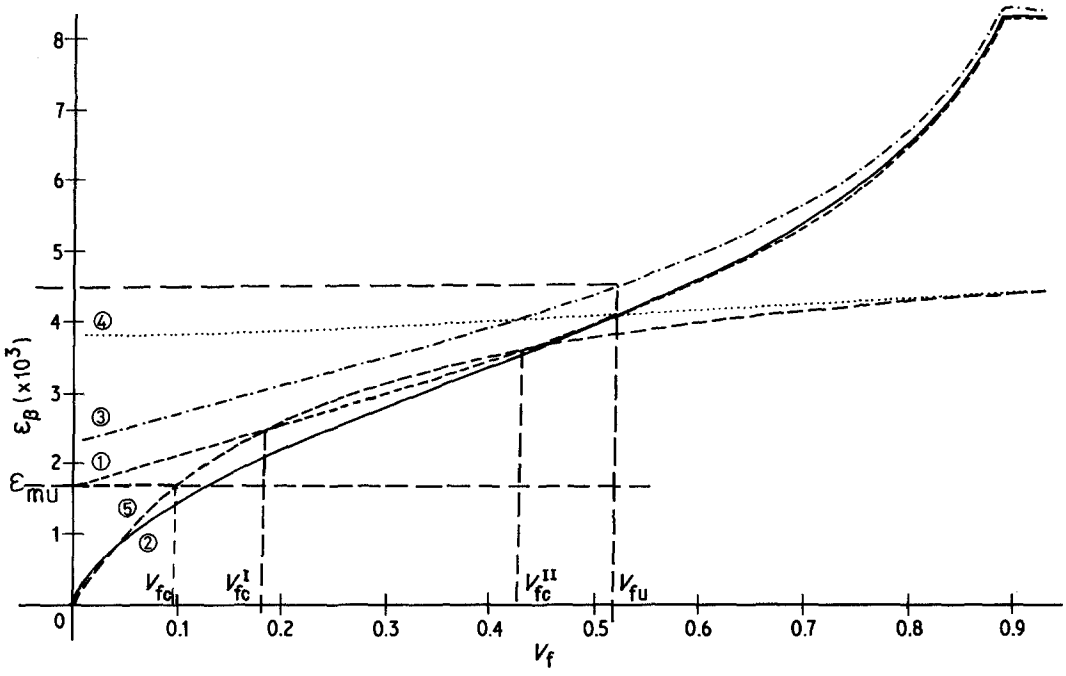

Figure 9 Illustrating the change in composite strain, ϵ_β, with fibre volume fraction, V_f, at which various failure processes occur. ($\tau = 10\,\mathrm{MN\,m^{-2}}$, $G_c = 20\,\mathrm{J\,m^{-2}}$).

Curve 5 represents the limiting condition that the load carried by the composite at the indicated failing strain of the matrix cannot be supported by the fibres alone. The intersection of Curve 5 with Curve 1 therefore gives the lower bound for the onset of multiple matrix cracking, V_{fc}^{I}, since, at higher fibre volume fractions, unstable extension of the matrix cracks occurs before the total strain (and load) applied to the composite exceeds the load which can be supported by the fibres. Note that in the absence of any matrix strengthening, by the inhibition of the growth of matrix cracks, matrix failure will occur at ϵ_{mu} and the onset of multiple matrix cracking will occur at a lower value of V_{fc}, i.e. the fibre volume fraction when Curve 5 crosses ϵ_{mu}.

The position of V_{fc}^{I} will, of course, depend on the physical characteristics of the particular composite system.

Multiple matrix cracking would be expected for this system at increasing fibre volume fractions until Curve 1 again crosses Curve 5 at V_{fc}^{II}. The failing strain of the matrix has now been increased to such a degree by stabilizing pre-existing cracks that the additional load which the reinforcing fibres have to support after failure of the matrix causes them to fail in turn. Hence, V_{fc}^{II} represents an upper bound for multiple matrix cracking. The strength of the composite will increase as indicated by Curve 1 with increasing fibre volume fraction beyond V_{fc}^{II}. The failure process now occurs by single fracture and is initiated by the propagation of the matrix crack followed by failure of the crack-bridging fibres.

Curve 4 in Fig. 9 represents the strain carried by the composite when the central fibre bridging the matrix crack reaches its failing strain. For the particular composite system considered this condition is not relevant over the multiple matrix fracture range because it occurs at a higher composite strain, ϵ_β, than that required for failure of the matrix. Composite failure as a consequence of this mechanism cannot occur until Curve 4 cuts Curve 1. This will precipitate single fracture of the composite at V_{fu}, a higher fibre volume fraction than V_{fc}^{II} the upper limit for multiple fracture. Failure will now be initiated by the fracture of the central crack-bridging fibre which, at higher fibre volume fractions, occurs at a lower composite strain than that at which matrix cracks propagate. The strength of the composite at fibre volume fractions greater than V_{fu} will now be controlled by Curve 4. It will be noted that the failing strain of the composite, by whatever fracture mechanism, is according to this analysis always less than the intrinsic failing strain of the fibres.

The curves shown in Fig. 9 and discussed so far

relate the bulk strain carried by composite ϵ_β to the volume fraction of reinforcing fibres and set limits for various failure sequences. Curve 3 refers specifically to the strain carried by the central crack-bridging fibre for values of ϵ_β at which the matrix cracks become unstable. If this is less than the failing strain of the fibres, ϵ_{fu}, composite fracture cannot be *initiated* by fibre failure. Note however, as discussed above, fibre failure can be caused *after* matrix fracture and Curve 5 defines a boundary condition for this. Where Curve 3 rises to the failing strain of the fibres ϵ_{fu} composite failure will be initiated by fibre failure and not by matrix failure. This occurs as previously discussed at the fibre volume fraction V_{fu}.

Curve 2 in Fig. 9 shows the enhanced matrix failure strain predicted by the ACK theory for this particular system. This theory also predicts a range of fibre volume fractions over which multiple matrix fracture would be expected and this is defined by the range of fibre volume fractions within which Curve 2, (indicating the matrix failure strain) lies below Curve 5, (indicating the composite strain below which the reinforcing fibres are able to support all of the load applied to the composite system). Note that this theory also predicts an upper limit of fibre volume fraction at which multiple matrix fracture is replaced by single fracture because the fibres cannot support the total load following failure of the matrix.

3.4. Correlation with experimental data

Experimental data on a number of fibre reinforced ceramic composite systems have been reported (see for example [3–5, 9, 10]. Glass fibre reinforced plaster, another example of a brittle matrix composite, is in extensive commerical use. Most of the systems studied incorporate random fibre arrays, but experimental data on unidirectionally reinforced carbon fibre borosilicate glass (pyrex) is available [1–5]. These studies have dealt with a wide range of fibre volume fractions and an attempt is made below to compare those experimental observations with the predictions of the theory outlined above.

Although experimental data on matrix cracking in this composite system is available, specific physical composite characteristics are not well defined. The interfacial shear strength between the carbon fibres and the hot-pressed glass powder matrix appears to be developed by the mechanical keying of fibre surface irregularities. From observations of the lengths of fibres protruding from the fracture surfaces Phillips *et al.* [3] deduce interfacial shear strength, τ, less than $27\,MN\,m^{-2}$. A value greater than $4\,MN\,m^{-2}$ was obtained from the observed average crack spacing when multiple cracking developed in the matrix whilst interlaminar shear stress values between 44 and $71\,MN\,m^{-2}$ were measured. Phillips [11] deduced values of τ ranging from 16.5 to $35.4\,MN\,m^{-2}$ and discussed the problems pertaining to the direct measurement of the fibre–matrix interfacial shear strength in this system [12]. The effective stress intensity factor for centre-notched specimens i.e. the cracks propagating parallel to the fibre direction, was also calculated. These calculations are, however, not directly applicable to the analysis presented here since the crack was not bridged over its entire length by fibres. Aveston *et al.* [5] assumed values of τ of 55 and $5\,MN\,m^{-2}$ for the carbon fibre pyrex glass system in comparing the experimental data with theoretical predictions of matrix cracking. As discussed by Phillips *et al.* [3] the elastic modulus of the matrix is influenced by the degree of porosity in the hot-pressed glass powder matrix. This factor may also influence the size of matrix flaws present in the composite particularly at high fibre volume fractions where considerable matrix porosity is observed. The tensile strength of the hot-pressed borosilicate glass matrix has usually been assumed to have a value of about $100\,MN\,m^{-2}$. The properties of the carbon fibres used were known with rather greater precision but the distribution of fibre flaws in terms of severity and separation are unknown. Some degree of fibre misalignment is also present and these factors will influence the failure processes in the composites to some extent. Further data on composite systems composed of various types of carbon fibres in a borosilicate glass have been reported by Prewo and Bacon [4] but numerical data on interfacial shear strengths was not reported.

Carbon fibre reinforced glass systems have been tested in flexure either in three-point or four-point bending. The load–deformation curve shows a change in slope which is ascribed to the development of transverse matrix cracks. The measurement by this means of the surface strain of the composite at which the first matrix crack occurs therefore presents major experimental difficulties. A further problem arises as a consequence of the

variability of fibre distributions and alignments. According to the analysis put forward here a matrix flaw of a particular size would be expected to propagate at a lower composite strain in a region of low fibre concentration compared with a region containing a high fibre volume fraction.

Various values of the work of fracture of hot-pressed borosilicate glass powder are reported in the literature. Aveston, Cooper and Kelly [5] assumed a value of $G_{ic} = 2\gamma_m$ of $8\,J\,m^{-2}$. Sambell *et al.* [1] assume a matrix work-of-fracture of $3\,J\,m^{-2}$. The effective work-of-fracture of the matrix in the composite will depend on the degree of irregularity of the matrix fracture surface, which from Sambell *et al.* [1] appears to be appreciable, and in the degree of localized multiple cracking which might be expected as a consequence of the matrix porosity and the presence of fibres. Hence, there is a measure of uncertainty in the value to ascribe to the matrix work-of-fracture.

Appreciable tensile thermal stresses are developed in the carbon fibre borosilicate glass composite system due to the different amounts of thermal contraction experienced by the fibres and the matrix on cooling to room temperature. This in turn will depend upon the viscosity–temperature relationship for the matrix and the rate at which the sample is cooled to room temperature after fabrication. Phillips *et al.* [3] take the temperature at which the glass matrix becomes effectively an elastic solid at 500° C above room temperature. After cooling to room temperature the fibres will be carrying a compressive strain ϵ_f and the matrix a tensile strain ϵ_m. On the basis of a simple balance of forces between fibres and matrix therefore

$$E_m V_m \epsilon_m + E_f V_f \epsilon_f = 0. \quad (13)$$

Hence,

$$\epsilon_m = \frac{\Delta T}{E_c} [E_f V_f (\alpha_f - \alpha_m)], \quad (14)$$

where ΔT is the temperature range (500° C) and α_f and α_m are, respectively, the thermal expansion coefficients of fibres and the glass matrix. Phillips *et al.* [3] quote $3.3 \times 10^{-6}\,°C^{-1}$ and $0.4 \times 10^{-6}\,°C^{-1}$ for α_m and α_f.

The tensile thermal stresses developed in various carbon fibre borosilicate glass matrix systems, ϵ_{mth}, calculated on the basis of the above argument, are shown in Table I. Also shown are the strain values, ϵ_β, at which matrix crack would be expected to propagate, in the absence of any thermal pre-stress, from the data given in Fig. 6. This assumes two alternative values of τ (50 and $10\,MN\,m^{-2}$), a matrix work-of-fracture of $8\,J\,m^{-2}$ and the presence of intrinsic matrix flaws perpendicular to the fibres and 37.2 μm long. (The analytical model used is of course two-dimensional.) As a consequence of the thermal stresses the composite strain at which matrix cracks propagate would be expected to fall as the fibre volume fraction increases. According to the model the effect of the crack-bridging fibres outweighs this effect for interfacial shear strengths of $50\,MN\,m^{-2}$ and the composite strength is predicted to increase for increasing fibre volume fractions (Table I). For composites with interfacial shear strengths of $10\,MN\,m^{-2}$ the thermal stress effect is almost balanced by the inhibition of crack growth in the fibres. For the higher shear stress value the results predicted from the theory are in tolerable agreement with the experimental data with the exception of the sample containing a fibre volume fraction of 0.293.

Phillips *et al.* [3] noted the unusually high experimental value of matrix cracking strain for this particular specimen. They suggested that a maximum cracking strain value could exist because the beneficial effect of increasing fibre volume fraction could be opposed by the associated increasing matrix porosity. However the data presented shows substantially constant matrix porosity values up to fibre volume fractions of 50%. Sambell *et al.* [1] noted the relatively low ultimate flexure strengths of the nominally unidirectionally reinforced composites compared with the values which would have been expected, $\sigma_f V_f$, from the known initial fibre strengths $\sim 2000\,MN\,m^{-2}$. They ascribed the reduced strengths to fibre misalignment and damage during manufacture. Similar comparatively low flexure strengths were observed by Prewo and Bacon [4] (see Table I), but the ultimate flexure strengths of most of the composites tested increase with increasing fibre volume fraction. The ratio between the composite ultimate tensile strength and the apparent point of deviation in the load–elongation curve does not exceed about 0.5 with the exception of the particular sample having a fibre volume fraction of 0.293 (Table I) where the ratio is about 0.8.

The theory of matrix crack instability considered here deals with a sheet of composite material containing a through crack, subjected to a

TABLE I

Volume fraction of carbon fibre (V_f)	Carbon fibre strength (σ_f) (MN m^{-2})	Porosity as a % of matrix	Mean flexural strength (MN m^{-2})	$\sigma_f V_f$	Mean bendover stress of composite (σ_β) (MN m^{-2})	Mean flexural strength (σ_β) (GN m^{-2})	Elastic modulus of composite (E_c) (GN m^{-2})	ϵ_{mth}	ϵ_β (τ = 50 MN m^{-2})	ϵ_β (τ = 10 MN m^{-2})	$\epsilon_\beta - \epsilon_{mth}$ (τ = 50 MN m^{-2})	$\epsilon_\beta - \epsilon_{mth}$ (τ = 10 MN m^{-2})	ϵ experimental
0.229	2000	3.8 ± 0.6	410	458	159	0.39	110	0.001 36	0.002 89	0.001 9	0.001 53	0.000 54	0.001 4
0.233	2000	3.7 ± 0.6	480	466	136	0.283	115	0.001 32	0.003 0	0.001 9	0.001 68	0.000 58	0.001 2
0.293	2000	5.1 ± 0.7	560	586	454	0.81	130	0.001 47	0.003 3	0.002 2	0.001 83	0.000 73	0.003 5
0.402	2000	4.2 ± 0.8	680	804	338	0.497	160	0.001 6	0.003 94	0.002 5	0.002 34	0.000 9	0.002 1
0.514	2000	5.8 ± 1.0	700	1028	191	0.273	192.5	0.001 74	0.004 74	0.002 76	0.003	0.000 9	0.001
0.594	2000	35.4 ± 1.5	310	1188	247	0.79	200	0.001 94	0.005 4	0.003 16	0.003 46	0.001 2	0.000 8
0.5*	2700*	–	590*	1350*	360*	0.61*	200*	0.001 62*	0.004 73*	0.002 7*	0.003 11*	0.001 08*	0.001 8*

*Data from Prewo and Bacon [4].

uniform tensile load in the fibre direction and in which the fibres are uniformly distributed. None of these assumptions are strictly true for composites tested in bending. In particular the fibres in many of the samples have highly non-uniform distributions. In such circumstances matrix cracks would be initiated in regions of low fibre concentration and be arrested as the crack tip propagated into regions of high fibre concentrations. Phillips *et al.* [3] observed the presence of stable matrix cracks of finite length in carbon fibre pyrex glass composites. The presence of individual cracks would provide a convenient means of testing the theory put forward here. If sufficiently long, the effect of any non-uniformity of fibre distribution along the length of the crack would be largely eliminated, and the crack length and the surface strain, ϵ_β, at which instability occurs would be measurable directly. Fig. 7 illustrates the relationship between the length of a matrix crack and the strain at which it becomes unstable. Furthermore, the analytical model used here could be modified quite straightforwardly to deal with any arbitrary distribution of fibres along the matrix crack by inserting appropriate values of V_f for the separate parallel segments into which the elliptical zone around the crack is divided in computing the energy release rate and energy absorption rate during crack extension (see Section 2).

3.5. Application of the theory to the design of composite systems of potential technological value

Composite systems utilizing either a polymeric or an aluminium matrix have been in commerical use for some time but have been limited to temperatures of about 300° C because of the characteristics of the matrix. As a consequence interest has now been focussed on silicate glass and ceramic matrix systems as a possible route to the development of composites with higher temperature capabilities. Work on silicon carbide reinforced glass [9] and alumina fibre reinforced glass [10] has recently been published.

The energy absorbing capability of the composite can be enhanced over that of the matrix alone by two different mechanisms. The first of these is associated with multiple matrix cracking. This is shown to particular advantage in the carbon fibre reinforced glass system [3]. The second energy absorbing mechanism is associated with the frictional energy losses occurring as discontinuous fibres are extracted from the matrix during separation of the crack faces. The experimental data shows, and the theory set out in Section 2 predicts, that large numbers of relatively short stable matrix cracks can be formed by the first mechanism if the fibres are non-uniformly distributed. The numerical calculations of the mechanics of matrix crack propagation, set out in Section 3 above, indicate the conditions under which multiple matrix cracking would be expected for a uniform fibre distribution. This analysis shows that the fibres will not modify significantly the mechanics of matrix crack propagation unless their diameters are small and their interfacial shear strengths fairly high.

Conversely the second energy absorbing mechanism occurring, as fibres are extracted from the matrix, becomes more important as the fibre diameter is increased and as the interfacial shear strength value is reduced. Hence it can be argued that composite systems containing fibres of very different diameters and interfacial shear strength values might offer advantages over composites containing only one type of fibre. The small fibres would be expected primarily to occupy the spaces between the large fibres and hence make possible higher fibre volume fractions in the composite and also generate a non-uniform distribution of fibres for matrix cracks having lengths comparable with the diameters of the large fibres. However, the small fibres would be effectively uniformly distributed for cracks having lengths greater than several large fibre diameters. Hence it is postulated that under some loading conditions irreversible energy loss would occur primarily by the generation of large numbers of small stable matrix cracks and under other loading conditions by the extraction of the large fibres from the matrix. Both types of fibres would, of course, reinforce the matrix in the conventional way.

Acknowledgements

This programme of work was supported by a research grant provided by the Science Research Council. The authors would like to thank Mr T. J. Dyson for his help with the computer graphics.

References

1. R. A. J. SAMBELL, D. H. BOWEN and D. C. PHILLIPS, *J. Mater. Sci.* 7 (1972) 663.

2. R. A. J. SAMBELL, A. BRIGGS, D. C. PHILLIPS and D. H. BOWEN, *ibid.* 7 (1972) 676.
3. D. C. PHILLIPS, R. A. J. SAMBELL and D. H. BOWEN, *ibid.* 7 (1972) 1454.
4. K. M. PREWO and J. F. BACON, Proceedings of the International Conference on Composite Materials, ICCM 2, AIME (1978) p. 64.
5. J. AVESTON, G. A. COOPER and A. KELLY, Conference on The Properties of Fibre Composites, National Physical Laboratory, Teddington, UK, 1971 (IPC Science and Technology Press, Guildford, 1971) pp. 15–24.
6. J. G. MORLEY and I. R. MCCOLL, *J. Phys. D: Appl. Phys.* 8 (1975) 15.
7. I. R. MCCOLL and J. G. MORLEY, *Phil. Trans. Roy. Soc.* **287** (1977) 17.
8. *Idem, J. Mater. Sci.* **12** (1977) 1165.
9. K. M. PREWO and J. J. BRENNAN, *ibid.* **15** (1980) 463.
10. J. F. BACON, K. M. PREWO and R. D. VELTRI, Proceedings of the International Conference on Composite Materials, ICCM 2, AIME (1978) p. 753.
11. D. C. PHILLIPS, *ibid.* 7 (1972) 1175.
12. *Idem, ibid.* 9 (1974) 1847.

Received 25 September and accepted 13 October 1980.